

PL-TR-97-2134

**DIFFERENTIAL ABLATION OF COSMIC DUST AND
IMPLICATIONS FOR THE RELATIVE ABUNDANCES
OF ATMOSPHERIC METALS**

William J. McNeil

Radex, Inc.
Three Preston Court
Bedford, MA 01730

September 15, 1997

Scientific Report #5

DTIC QUALITY INSPECTED 2

Approved for public release; distribution unlimited



**PHILLIPS LABORATORY
Directorate of Geophysics
AIR FORCE MATERIEL COMMAND
HANSCOM AIR FORCE BASE, MA 01731-3010**

19980317 066

This Technical Report has been reviewed and is approved for publication”


JOHN CIPAR
Contract Manager


LT COL FRANK ZAWADA
Branch Chief

This report has been reviewed by the ESC Public Affairs Office (PA) and is releasable to the National Technical Information Service (NTIS).

Qualified requestors may obtain additional copies from the Defense Technical Information Center (DTIC). All others should apply to the National Technical Information Service (NTIS).

If your address has changed, if you wish to be removed from the mailing list, or if the address is no longer employed by your organization, please notify PL/IM, 29 Randolph Road, Hanscom AFB, MA 01731-3010. This will assist us in maintaining a current mailing list.

Do not return copies of this report unless contractual obligations or notices on a specific document require that it be returned.

REPORT DOCUMENTATION PAGE

Form Approved
OMB No. 0704-0188

Public reporting burden for this collection of information is estimated to average 1 hour per response, including the time for reviewing instructions, searching existing data sources, gathering and maintaining the data needed, and completing and reviewing the collection of information. Send comments regarding this burden estimate or any other aspect of this collection of information, including suggestions for reducing this burden, to Washington Headquarters Services, Directorate for Information Operations and Reports, 1215 Jefferson Davis Highway, Suite 1204, Arlington, VA 22202-4302, and to the Office of Management and Budget, Paperwork Reduction Project (0704-0188), Washington, DC 20503.

1. AGENCY USE ONLY (Leave Blank)	2. REPORT DATE 15 September 1997	3. REPORT TYPE AND DATES COVERED Scientific Report No. 5	
4. TITLE AND SUBTITLE Differential Ablation of Cosmic Dust and Implications for the Relative Abundances of Atmospheric Metals		5. FUNDING NUMBERS PE 63871C PR 7659 TA GY WU AG Contract F19628-95-C-0106	
6. AUTHORS W. J. McNeil		8. PERFORMING ORGANIZATION REPORT NUMBER RXR-970901	
7. PERFORMING ORGANIZATION NAME(S) AND ADDRESS(ES) Radex, Inc. Three Preston Court Bedford, MA 01730		10. SPONSORING / MONITORING AGENCY REPORT NUMBER PL-TR-97-2134	
9. SPONSORING / MONITORING AGENCY NAME(S) AND ADDRESS(ES) Phillips Laboratory 29 Randolph Road Hanscom AFB, MA 01731-3010 Contract Manager: John Cipar/GPD		11. SUPPLEMENTARY NOTES	
12a. DISTRIBUTION / AVAILABILITY STATEMENT Approved for Public Release Distribution Unlimited		12b. DISTRIBUTION CODE	
13. ABSTRACT (Maximum 200 words) <p>Metals in the Earth's atmosphere are of interest and importance for several reasons. Emission lines from the sodium layer are used for wave front corrections in imaging space objects. The ionospheric metals present background contamination for remote sensing and tracking of space-born objects. Ionization during meteor showers may also interfere with communications. Although it is generally accepted that extraterrestrial material is the source of metals in the atmospheric, the relative abundances of mesospheric metals and ions present us with a conundrum. Lidar observations have consistently shown that the abundances of neutral metals in the atmospheric and the abundances of these metals in the meteoric material that falls to earth are significantly disproportionate. For example, the column density of neutral sodium is perhaps two orders of magnitude larger than that of calcium, while the abundances in meteorites are approximately equal. To complicate matters further, ion mass spectroscopy has shown that the abundances of the meteoric ions match reasonably well those in the meteorites. We present here a model that attempts to address these discrepancies. At the heart of the model is the concept of differential ablation, which suggests that more volatile metals sublime earlier in the descent of a cosmic dust particle than do the less volatile components. The modeling is carried out comprehensively, beginning with the heating and vaporization of the dust particles. The vaporization rate is computed as a function of altitude from an ensemble of particles to give a deposition function which is then injected into a fully time-dependent kinetic code which allows for vertical diffusion and includes diurnal dependence through both the models of the major atmospheric components and through transport of the ions due to electric fields. We model three different meteoric metals: sodium, magnesium and calcium. Results suggest that sodium ablates to a greater extent than does calcium and that it ablates at a substantially higher altitude. Both of these lead to a relative depletion of calcium, the first obviously so. We have found, too, that deposition at lower altitudes leads to more rapid conversion of the elemental metal into complexes and reduces column density. This appears to be the predominant mechanism for calcium reduction. We examine the behavior of the model in the thermosphere and mesosphere, comparing predicted results with measurements and finding reasonable agreement. We argue that the success of this model indicates that differential ablation is a key factor in the relative abundances of meteoric metals in the atmosphere.</p>			
14. SUBJECT TERMS Atmospheric metals, Atmospheric modeling, Meteor ablation, Differential ablation, Mesospheric chemistry		15. NUMBER OF PAGES 46	
17. SECURITY CLASSIFICATION OF REPORT Unclassified		16. PRICE CODE	
18. SECURITY CLASSIFICATION OF THIS PAGE Unclassified	19. SECURITY CLASSIFICATION OF ABSTRACT Unclassified	20. LIMITATION OF ABSTRACT Unlimited	

TABLE OF CONTENTS

1. INTRODUCTION	1
2. DEPOSITION PROFILES	4
3. THE DYNAMIC MODEL	16
4. RESULTS	27
5. SUMMARY	34
6. REFERENCES	36

Preceding Page Blank

LIST OF FIGURES

1. Vapor pressure curves determined from the *Fegley and Cameron* [1987] thermodynamic model for a melt of pure Na_2O (top) for the model used in sodium deposition (center curve) and magnesium deposition (bottom) 9
2. Curves showing the fraction of the vapor which is comprised of silicon containing species (dashes) and magnesium species (solid line) derived from the *Fegley and Cameron* [1987] model evaluated at 2000°K for an equal mixture of SiO_2 and MgO in the molten phase 11
3. Histories of 1(-5) gram sodium and magnesium particles as they descend through the atmosphere showing temperature in $^\circ\text{K}$ (top) and fraction of the initial mass of the particle remaining 13
4. Illustration of the velocity dependence of the fraction of mass ablated and the altitude of the ablation for a 1(-5) gram calcium dust particle . . 14
5. The deposition curves resulting from the differential ablation model for the three metals at incoming velocities of 12 km/sec (left) and 15 km/sec (right) 15
6. The model for neutral atmospheric components used in these calculations . 21
7. Removal rates for neutral metals computed from Eq(5) and Eq(6) and the rates in Table 2 for the two-component model 22
8. Comparison of the magnesium ion layer predicted by the model with the rate for Rxn(19) at 1(-30) (solid line), 1(-31) (dashed line), 1(-32) (dot-dash), and $0/\text{cm}^6\text{-sec}$ (dots) (top to bottom) as compared with published Mg^+ IMS [*Grebowsky et al.*, 1997] 24
9. Illustration of the primary mechanism for calcium depletion comparing the altitude of deposition of sodium (right) with calcium (left) as they relate to the altitude where the sink becomes dominant 30
10. Mesospheric ion and neutral layers resulting from a mixture of 2% fast and 98% slow meteoric dust particles taken at dusk 33

LIST OF TABLES

1. Relative Abundances of Meteoric Metals	2
2. Kinetics of the Two-Component Models	18
3. Model Column Densities	28
4. Parametric Study of Neutral and Ion Ratios	32

ACKNOWLEDGEMENTS

This work was performed under the careful guidance of Dr. Edmund Murad and Dr. Shu Lai, both of Phillips Laboratory. The success of this effort is due primarily to the excellent knowledge, guidance, and intuition provided to us by these researchers. Through the auspices of Dr. Murad and of Phillips Laboratory, especially through the USAF's "Window on Science" program, we have had the honor of conferring at length with many who are unequivocal leaders in the field of meteor astronomy and of atmospheric metal chemistry. We, including the above named government employees, are indebted to J. M. C. Plane of the University of East Anglia, UK, for his initial work on differential ablation and for sharing with us his results on the kinetics of atmospheric metals. We are also, as usual, indebted to D. A. Hughes of the University of Sheffield, UK, for sharing with us his considerable knowledge of cometary streams. Discussions with W. J. Baggaley of the University of Canterbury, Christchurch, NZ, on radio meteor observation techniques were extremely beneficial, as were discussions with W. D. Pesnell of Nomad Research, Inc., MD, on the formation and characteristics of the Earth's dust cloud. We are especially thankful to J. Grebowsky of NASA/Goddard for allowing us to use his collection of magnesium IMS measurements. Portions of this work were performed under USAF contract F19628-93-C-0023, in addition to the contract cited on page ii.

1. INTRODUCTION

Since the early optical studies of sodium D emission [e.g., Chapman, 1938; Blamont, 1953], the metallic species present in the Earth's atmosphere have been the subject of extensive research and modeling efforts. The development of the Lidar technique later allowed for detailed probing of the atmospheric sodium layer and variations therein with the seasonal and yearly cycles [e.g., Megie and Blamont, 1977]. Later, rocket-borne mass spectrometry [e.g., Kopp and Herrman, 1984; Aikin and Goldberg, 1973] began to reveal the details of the mesospheric metal ions as well. With the advent of satellite photometry, information on the structure and dynamics of thermospheric metals also became available [e.g. Gerard and Monfils, 1974, Gardner, et al., 1996]. In-situ satellite observations have confirmed the results of the optical measurements [e.g. Hanson and Sanatani, 1970, Grebowsky, et al., 1978, 1985]. The addition of Lidar data garnered for metals other than sodium [Granier, et al. 1989; Gardner, et al., 1993; Qian and Gardner, 1995] gave an impressive complement of information on neutral and ionized atmospheric metals.

As data from these sources began to accumulate, it became clear that an anomaly existed. It is generally accepted that the metals in the Earth's atmosphere arise primarily from the ablation of cosmic dust of extraterrestrial origin [Hughes, 1992]. Cosmic dust is, for the most part, composed of carbonaceous chondrites which are more or less uniform in relative metal content [Mason, 1971]. Table 1 lists some rough relative contents for three species that we will consider here, sodium, calcium and magnesium, along with rough numbers for measured mesospheric abundances. The data are by relative mole fraction and show that magnesium is about twenty times more abundant than are the other two, with sodium and calcium of about equal abundance. Lidar observations, which cannot be made from the Earth for magnesium due to the strong absorption of the Mg-I 285.2 nm line by the Earth's ozone layer, show that neutral sodium in the mesosphere is approximately two orders of magnitude more abundant than calcium, despite the fact that the meteoric content is approximately equal. Turning to the mesospheric ions, though, we see that the column densities are again in at least rough agreement with the meteoric content. The measurement of ion densities in the mesosphere is difficult and the numbers presented admittedly contain a good deal of uncertainty. Still, the disagreement between the ion and neutral abundances is clear.

TABLE 1. Relative Abundances of Meteoric Metals				
Material	Source of Data	Na/Ca	Mg/Ca	Mg/Na
Cosmic Dust	Examination of meteor falls ¹	1	20	20
Mesospheric Neutrals	Lidar Observations ²	100	???	???
Mesospheric Ions	Rocket Ion Mass Spectroscopy ³	3	21	8

- ¹ Approximate values by number are taken roughly from *Mason* [1971]. These numbers are representative of Chondrites which account for about 85% of all meteor falls.
- ² Value for calcium-to-sodium taken from *Qian and Gardner* [1995] represents column density. Values involving magnesium are unknown due to the inability of the Mg I line to penetrate the Earth's ozone layer.
- ³ All values for ion column density are taken from the data of *Zbinden, et al.* [1975] and are the result of our own reduction of results presented there, taken during the Geminid Meteor Shower of 1971. The ratios are essentially echoed by several other authors, *e.g. Kopp* [1997].

This situation is rendered even more tantalizing by the fact that the neutral sodium and calcium layers are not much different from each other in shape or position [see *e.g. Qian and Gardener, 1995*] nor is the chemistry of neutral sodium and calcium sufficiently different to explain the depletion, as concluded by *Plane and Helmer* [1994]. *Plane* [1995] concluded that in order to explain the depletion of calcium in the mesosphere, one must assume that the ratio of ablated sodium to calcium is about thirty-six. In other work on magnesium, *Plane and Helmer* [1995] conclude that the ratio of sodium to magnesium flux from meteoric ablation must be about 2:1, which amounts to approximately the same depletion level. This depletion in magnesium amounts to a factor of about forty relative to the meteorite abundance ratios.

In this report, we attempt to model the process of differential ablation, the idea that sodium ablates differently from calcium or magnesium during the descent of a cosmic dust particle. We then examine the effect on the relative metal abundances. The approach begins with some rather crude assumptions about what the cosmic dust particles are like and how they vaporize. From these simplistic models, vapor pressure curves are computed following *Fegley and Cameron* [1987] which are then used in formulae [*Love and Brownlee, 1991*] for the evaporation rates of the metals. An ensemble of particles is then tracked through descent following a mass distribution

representative of cosmic dust [Hughes, 1991] to arrive at an ablation profile for each metal species. This method follows McNeil, et al. [1995] and, when combined with the differential ablation, gives deposition profiles which are different for each metal. While the ablation model is admittedly simplistic, it seems adequate to demonstrate that differential ablation is a primary factor in calcium depletion.

That the differential ablation or fractionation (as metallurgists would say) of meteoroids does in fact take place is evidenced by chemical analysis of cosmic dust spherule collected from deep sea sediments, polar ice and from the stratosphere. These analyses show clearly that the more volatile elements such as Na and K are nearly absent [Papanastassiou, et al., 1983; Brownlee, et al., 1997]. The depletion is almost certainly due to the differential ablation of the volatile elements during atmospheric entry and melting. These particles, as opposed to the larger meteorites, the interiors of which likely do not melt, are precisely those which contribute most to the metal layers in the atmosphere. Therefore, it makes sense that differential ablation should have a strong impact on the relative abundance of atmospheric metals. It is important to realize, when considering the process of differential ablation, that the process applies to small cosmic dust particles with diameters below, say, 1 mm. These particles could be expected to heat, melt, and ablate uniformly. This is as opposed to larger particles which would undergo what one might term "surface ablation", whereby only the surface of the particle is melted and ablation persists at a rate in proportion to the meteoric abundance of metallic species. These larger particles, although the most spectacular to visual observers, are not those which dominate the dynamics of the mesospheric metals.

In order to compute metal atom and ion profiles and column densities for comparison with measurements, the ablation profiles are used in a model for atmospheric metals following McNeil, et al. [1996]. The model extends work on the mesospheric neutral layers [McNeil, et al., 1997] and includes fully time-dependent ablation and diffusion, transport of the ions *via* electric field drift, and a reasonably comprehensive set of chemical reactions. The model allows for only two species, atomic ion and neutral. However, source and sink rates are computed for neutrals and ions considering branching between recycling and destruction. Multi-component equivalents have been developed to confirm the validity of the two-component approach.

In the following section, the vaporization model used to calculate the ablation rates of the metals is described and the equations and the initial mass distribution function used to compute the deposition profiles are presented. Following that, the two-component models used to evaluate the deposition profiles are discussed. Next, parametric studies on the sodium to calcium ratio variation with cosmic dust particle velocity are carried out, with the finding that several combinations give reasonable agreement with experiment. It is admitted at the outset that neither the measurements nor the information necessary for accurate modeling are at this point well known. Therefore, one should not expect profound agreement, nor should one fail to allow for the possibility that some of the agreement, where it exists, may be fortuitous. Based on the results of this modeling, however, it is submitted that differential ablation is a plausible mechanism for controlling the abundances of atmospheric metals.

2. DEPOSITION PROFILES

As dust particles fall through the atmosphere, friction causes them to heat and evaporate. For any given dust particle, the rate and altitude at which deposition begins and ends depends most strongly on three factors. The first of these is the size of the particle. The second is the initial extraterrestrial velocity of the particle relative to the Earth's velocity. The third is the rate of evaporation of the material as a function of the particle's temperature. A deposition profile, in the context of this work, will be the rate of evaporation as a function of altitude for a particular metal species; Na, Ca or Mg. In order to compute one of these, we need to specify a distribution of particle sizes, particle velocities, and a temperature dependent evaporation rate. These three things, along with equations describing the deceleration and heating of the of the particles and along with a model for atmospheric density will allow us to calculate a profile. We turn first to the equations describing the descent of the particle which are taken directly from *Love and Brownlee* [1991]. The equations make clear the impact of the particle's vapor pressure upon its evaporation.

First, the deceleration of a particle due to collisions with air molecules is computed by equating the momentum change of the dust particle with the mass of air encountered times the particle's velocity, resulting in the following formula.

$$\frac{dv}{dt} = \left(-0.75 \frac{\rho_a v^2}{\rho r} \hat{v} + g \right) \quad (1)$$

In Eq(1), v is the particle velocity, ρ is the particle density taken to be 3.2 g/cc, ρ_a is the density of the air which is derived from the US Standard Atmosphere for solar minimum tabulated by *Kelley* [1989], r is the particle radius, and g is the gravitational constant. The temperature of the dust particle is then computed by equating the energy input from collisions with the air molecules with the radiative cooling plus the energy loss through evaporation.

$$\frac{1}{2} \rho_a v^3 = \epsilon \sigma T^4 + H_f C p_v \sqrt{M/T} \quad (2)$$

In Eq(2), ϵ is the particle's emissivity taken to be unity, σ is the Stefan-Boltzmann constant, T is the particle's temperature, H_f is the latent heat of fusion taken to be 6.05(10) ergs/g, C is a conversion factor equal to 4.377(-5) for a spherical particle, p_v is the vapor pressure, and the molecular weight is M . Eq(2) is solved iteratively at each time step for the temperature.

It is then assumed that the mass loss is due to evaporation of a molten liquid, for which the rate was given by *Langmuir* [1913] as

$$\frac{dm}{dt} = 4 \pi r^2 C p_v \sqrt{M/T} \quad (3)$$

With these equations, the time history of a single particle can be tracked during descent through the atmosphere.

There are four additional pieces of information needed in order to proceed. One of these is the initial angle of attack of the cosmic dust particle. We have found that, except for those particles which impact the atmosphere at angles so shallow that they skip out of the atmosphere entirely [*Love and Brownlee*, 1991] the angle of attack makes very little difference in either the amount or altitude of deposition. The effect

of the attack angle, when the angle is reasonably deep, is to shorten slightly the deposition region for each particle in the distribution, but each particle will begin ablation at the same altitude regardless of angle. A change in angle is not equivalent to a change in the incoming velocity. Therefore, we have fixed the attack angle at 45° for all of these calculations. A second necessity is a distribution of cosmic dust particle sizes. We have retained the distribution used in earlier work [McNeil, *et al.*, 1995] for this purpose; this estimate is based on data obtained by Love and Brownlee [1993] and on the analysis by Hughes [1995]. It is worthwhile for what follows to discuss the ablation behavior of this distribution. Cosmic dust particles become less and less frequent as their masses increase. On the other hand, very small particles will not ablate at all because they reach terminal velocity without attaining a temperature above the melting point. Therefore, the relative contribution to ablation as a function of mass shows a peak. In the ablation models used here, this peak is near 1(-6) grams (by 1(-6) is meant 1×10^{-6} , and similarly throughout). The assumed distribution is slightly more populous at higher mass, so that the median particle contributing to the metal layers is nearer 1(-5) grams. Said another way, the major contributors to the atmospheric metal layers are cosmic dust particles which are quite small. In our model, about 95% of the contribution comes from particles between 1(-8) and 1(-3) grams. This is in stark contrast to the meteoroids which give rise to the visual phenomenon of shooting stars, where the typical limiting acuity of the human eye is to bodies of greater than 10 mg.

A third parameter is the velocity of the incoming meteoric particle. Velocity distributions are presented by Hughes [1975] showing a range between 11 km/s, which is the escape velocity of a stationary dust particle in orbit with the Earth from Earth's gravitational field, and about 70 km/second. Hughes presents two distributions, one of which is for visual meteors which are the larger and/or faster particles and the other which is for meteors measured by radio echo from ionization trails. The visual meteors show a peak at around 15 km/s while the radio meteors show a peak near 30 km/s. As pointed out by Hughes, however, the radio echo technique is not capable of detecting smaller dust particles with low velocities, so that the actual number of slow, small dust particles is essentially unknown [Hughes, 1997]. This is especially significant since the majority of the particles contributing to the metal layers are less than 1(-4) grams in mass and are therefore at the low end of the radio meteor population. We will find that the velocity of the incoming dust particle is critical in determining the relative neutral metal abundances and, therefore, we will leave the

incoming velocity as a variable parameter, noting only that there is reason to suspect that there may be a large number of particles in the 1(-6) to 1(-3) gram range which have low geocentric velocities [Hughes, 1975], and which are essentially invisible to radio echo.

The final parameter needed to proceed is the vapor pressure p_v for use in the above equations. It is at this point that the differential nature of the ablation is introduced into the model. *Fegley and Cameron* [1987] have developed a model of the vaporization and fractionization (which might be the cosmologist's term for differential ablation) of a molten silicate chondritic magma in an attempt to explain Mercury's unusually high density. Their treatment is, in many respects, appropriate for the problem at hand, if we should assume that cosmic dust particles melt completely early in the ablation process, that the vapor and melt are in thermodynamic equilibrium at all times and that the particles are small enough so that diffusion allows the melt to remain homogeneous at all times. *Love and Brownlee* [1991] examine the problem of melting and present curves showing melt and no melt regimes for various out-of-atmosphere velocities. For 20 km/sec at 45° entry angle, particles above about 20 μm in diameter are predicted to melt. This corresponds to a mass of about 1(-8) grams and as discussed in the preceding paragraph, the contributors to the atmospheric metal layers are overwhelmingly above this size limit. Therefore, it would seem that melting should be assured for these particles.

The other two requirements are more difficult to quantify. As to thermodynamic equilibrium, we note that the ablation process takes about one second for a typical dust particle, which seems long enough for the equilibrium assumption to become valid at temperatures above 1000 K and pressures of several tenths of an atmosphere. As to the issue of diffusion, we note again that the particles contributing to the metal layers are overwhelmingly small and so it feels correct to assume that the more volatile elements should have little trouble reaching the surface. In any case, the model for differential ablation employed here is admittedly crude. It is our intent only to introduce a simple mechanism which allows the sodium to ablate preferentially and to show that this produces a substantial depletion in calcium relative to sodium.

Briefly, the *Fegley and Cameron* [1987] model uses thermodynamic equilibrium to compute the vapor pressure and composition of the vapor above a melt which is a combination of metal oxides, such as Na_2O , CaO , MgO , SiO_2 , etc. We will omit the

detailed equations and describe only the general approach and the adaptations we have made for the problem at hand. The original *Fegley and Cameron* model employs a total of eleven metal oxides. Their method begins by choosing a set of mole fractions for the metal oxides in the magma, then solving for thermodynamic equilibrium giving the relative abundances of the metals in the vapor phase. This also allows for the vapor pressure above the melt to be computed. A small amount of each metal oxide is then removed from the melt corresponding to the relative amount in the vapor and the process is repeated again and again. What results are curves showing the composition of the vapor and melt as the vaporization progresses. What is striking about the curves presented in *Fegley and Cameron* [1987] is that the vaporization of the sodium oxide is complete within the first 5% of the mass loss. Also, during this period, the vapor above the melt is almost completely Na, O and O₂. As obviously follows, the change in composition of the melt with respect to the other metal oxides is minimal during the sodium vaporization. These features tempt one to consider a very simple model for sodium ablation, that the sodium comes off independently of any of the other metal in the meteoroid.

To implement this model, we need to compute a vapor pressure. This has been done by exercising the *Fegley and Cameron* [1987] technique for a mixture containing 49% SiO₂, 49% MgO and 2% Na₂O. The Fegley and Cameron model is also evaluated for a pure Na₂O melt. These vapor pressures were evaluated at several temperatures and were fit to a classic form for vapor pressure laws given in Eq(4).

$$\log_{10} p_v = A + B/T \quad (4)$$

The resulting curves are shown in Figure 1. The crux of the sodium ablation model is, then, that the sodium comes off first while the rest of the cosmic dust melt remains intact. This is consistent with experimental results which, while perhaps not precisely duplicating the cosmic dust ablation process, argue for the early evaporation of sodium. *Notsu, et al.* [1987] examined the volatilization of meteorites by heating bulk samples in vacuum and analyzing the residual fraction at various stages of the heating. Their plots show quite dramatically that Na₂O is eliminated from the sample very rapidly and that the rest of the sample is basically unaltered in content during the removal of the sodium. The experimental curves themselves are strikingly similar to the theoretical Fegley and Cameron curves. It is not unreasonable, therefore, to assume that sodium

may be completely removed from the dust before ablation of the less volatile metals even begins.

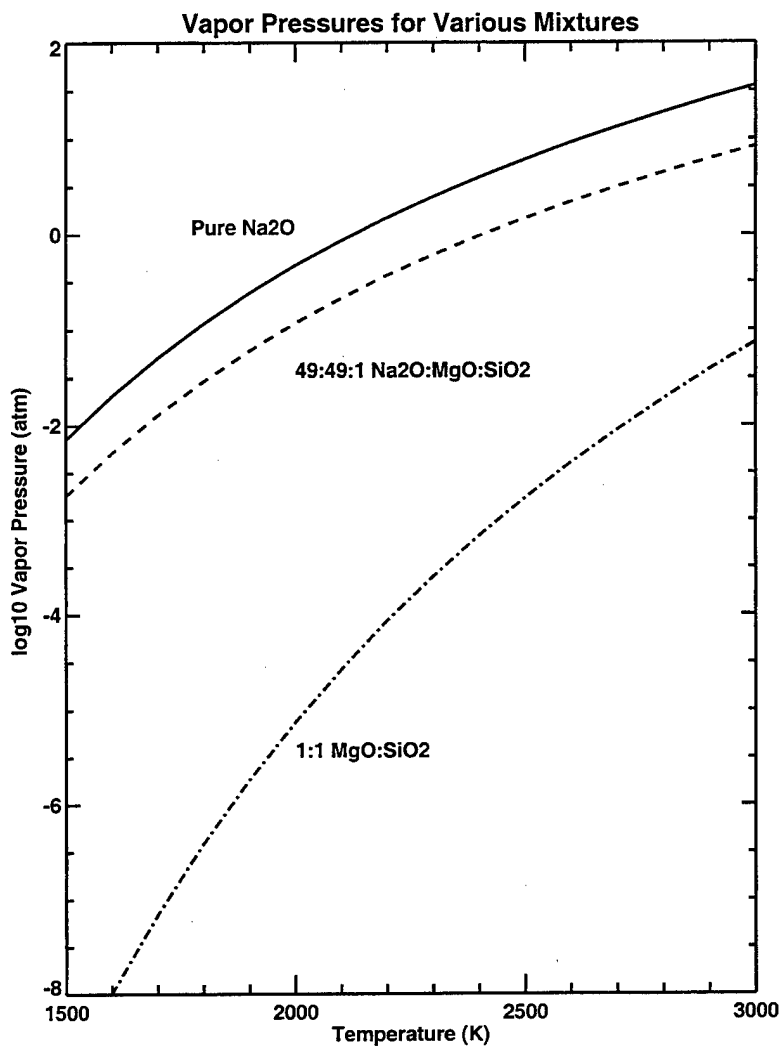


Figure 1. Vapor pressure curves determined from the *Fegley and Cameron* [1987] thermodynamic model for a melt of pure Na₂O (top) for the model used in sodium deposition (center curve) and magnesium deposition (bottom).

In order to treat more correctly the ablation of the sodium from the 2% Na₂O solution, a modification is needed in the *Love and Brownlee* [1991] formalism. Since the sodium makes up only 2% of the entire dust particle and since the remainder of the dust

particle is not being ablated during the ablation of sodium, it is assumed that the heat loss due to the sodium ablation is negligible. Therefore, the temperature in Eq(2) is computed as if the sodium were absent altogether. The mass loss of sodium is computed from

$$\frac{dm}{dt} = 4\pi r^2 p_v \sqrt{M/T} \frac{m_{Na}}{m_{Na,0}} \quad (5)$$

where p_v is the vapor pressure of the 48:48:2 solution. The size of the particle, however remains essentially unchanged during the evaporation of the sodium. To omit this modification would cause the particle to become too small too fast and would keep the temperature unrealistically low due to a too rapid heat loss through Eq(2). Said another way, the temperature and size of the particles are computed with Eq(1) through Eq(3) with a vapor pressure law for the 50:50 mix of magnesium and silicon, to be discussed next, while the evaporation of sodium is computed with the vapor pressure law of the 49:49:2 mix including the sodium and using Eq(5).

Turning next to the ablation of magnesium, we note that magnesium and silicon are the primary constituents by number density in chondritic material and that they are about equally plentiful. We have also noted from the plots in *Fegley and Cameron [1987]* that magnesium and silicon are also the most plentiful in the vapor by a factor of ten, down to the point where perhaps 5% to 10% of the original magma remains. Thus, it seems reasonable to treat the ablation of magnesium with a two-component system initially containing a 1:1 mixture of SiO_2 and MgO . The general idea is that, so far as the magnesium is concerned, the ablation takes place almost as if the other elements were not present at all. Although it seems to be legitimate to ignore the other species under these circumstances, we must still consider the relative amounts of magnesium to silicon in the vapor, which can and do change during the evaporation. Figure 2 shows the relative composition of the vapor as a function of the amount of material that has evaporated.

Except for perhaps the residual 5% of the dust particle, the difference between magnesium and silicon in the vapor is no more than 20%. Note that this difference increases with increasing temperature and that the 2000° K used for Figure 2 is the maximum temperature that our dust particle will attain. In keeping with the overall theme of this model, which is to represent differential ablation in some physically

meaningful yet simple way, we have chosen to ignore the differences in the vapor composition as the particle ablates. This means that, as with sodium, magnesium ablation can be represented with a single temperature dependent vapor pressure law. As with sodium, the results of the Fegley and Cameron treatment were fit to Eq(4). The lower curve in Figure 1 shows the result.

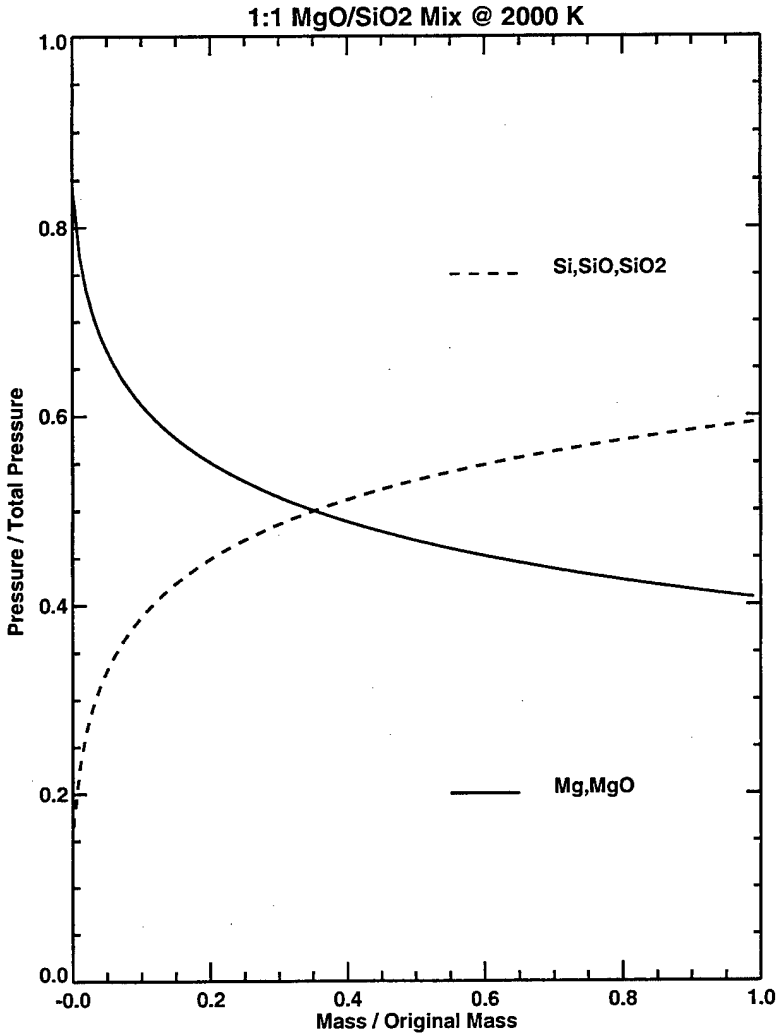


Figure 2. Curves showing the fraction of the vapor which is comprised of silicon containing species (dashes) and magnesium species (solid line) derived from the Fegley and Cameron [1987] model evaluated at 2000° K for an equal mixture of SiO₂ and MgO in the molten phase

The deposition of calcium is modeled by relation to magnesium. According to *Fegley and Cameron* [1987] magnesium and calcium in the vapor parallel each other well down to the 80% ablation point. This behavior is also seen in the *Notsu, et al.* [1978] experimental curves, where the relative abundance of CaO and MgO is approximately constant down to the point where about 90% of the meteor has vaporized. As dust particles pass the point of 80% ablated, it appears that they become rapidly enriched in calcium relative to magnesium. This is probably quite important to those who collect the remnants of these particles from the stratosphere, but it is of little consequence to the mesospheric metal layers. During the better part of the ablation process, calcium and magnesium appear to be coming off at rates proportional to their abundances. For this reason, and for the inherent simplicity of the approach, we have chosen to model calcium ablation with the same vapor pressure law as is used for magnesium.

It is instructive to examine in detail the time history of a single particle. The temperature and mass loss curves shown in Figure 3 are taken for a 1(-5) gram particle using both the sodium and calcium vapor pressure laws. Again, 1(-5) gram particles are the peak contributors to the atmospheric metal layers, according to this model. As expected, the temperature is the same for both the sodium and magnesium (or calcium) since we have neglected heat loss due to sodium ablation. As the bottom curves show, the sodium is completely ablated from the particle while the calcium has about 20% of the mass remaining when ablation ceases. It is also clear from the curves that the calcium ablates at a lower altitude than does the sodium. As will become clear, both of these properties will be important in determining the mesospheric abundances. Another parameter to consider is the effect of the initial velocity of the particle on the rate of ablation and the deposition height. Figure 4 shows the effect of this parameter for calcium. It is interesting that only the very slow particles show a significant mass fraction remaining after ablation. This is significant in that one can only obtain a relatively small depletion in calcium, perhaps a factor of 10 at best, through direct differential ablation. By direct differential ablation we mean the reduction attributable to left-over calcium in the unablated remnant dust particle. We will see as we complete the model that the altitude of ablation is another factor which contributes strongly to the depletion.

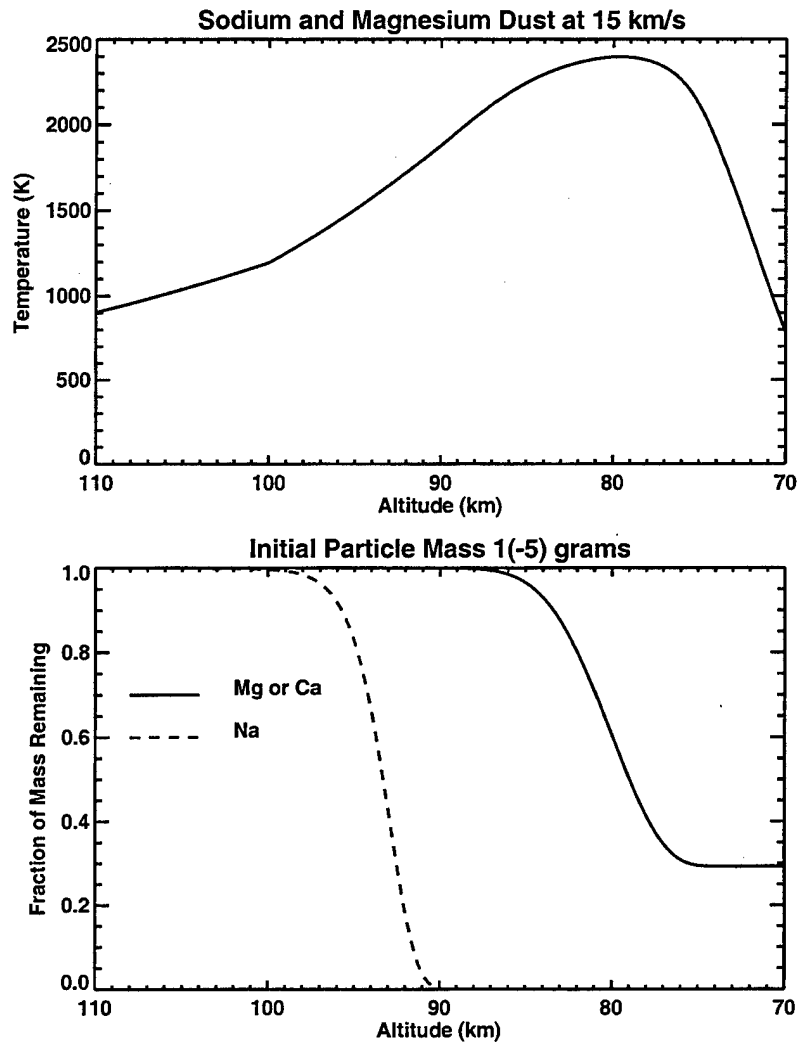


Figure 3. Histories of 1(-5) gram sodium and magnesium particles as they descend through the atmosphere showing temperature in °K (top) and fraction of the initial mass of the particle remaining.

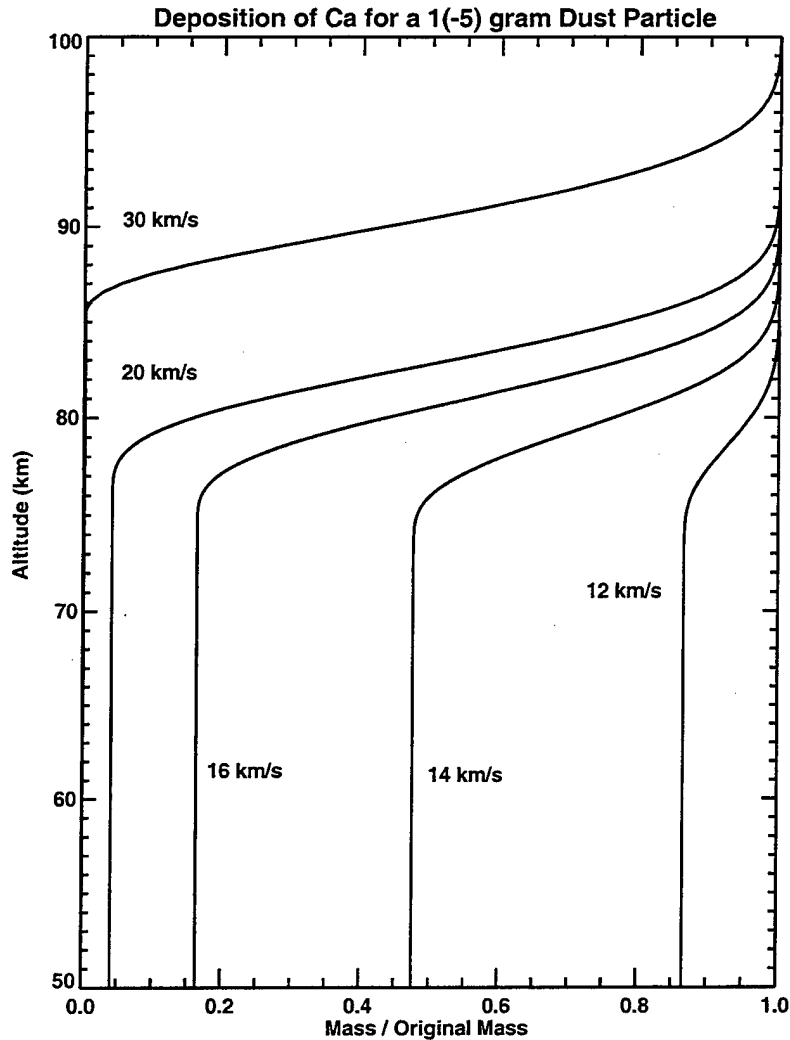


Figure 4. Illustration of the velocity dependence of the fraction of mass ablated and the altitude of the ablation for a 1(-5) gram calcium dust particle. The same curves would obtain for magnesium since it is modeled identically.

The computation of an ablation curve is carried out as in *McNeil, et al.* [1996] by selecting an ensemble of particles from the prescribed mass distribution, following these particles until they reach terminal velocity, and accumulating the deposited material in bins of 1 km size according to Eq(3). Of course, at this point, the deposition profiles will not be normalized to any sensible quantity. We normalize the sodium deposition profile to represent a total influx of 500 grams/sec of cosmic dust into the atmosphere. This number is from *Hughes* [1975] and is, of course, quite approximate. In these calculations, the deposition profiles are also subject to a scaling factor α which

is the same for all species and which can be used to control the overall column density, so that the value of 500 grams/sec is not relevant in the end. The magnesium and calcium deposition curves are normalized by the same factor as for sodium. This gives us deposition rates which are relative to sodium. We then scale up the deposition profiles for calcium and magnesium by the relative abundances of these metals to sodium in meteoric metals, taken to be 1:1 and 20:1 respectively. Deposition curves for incoming velocities of 30 km/sec and 15 km/sec are shown in Figure 5.

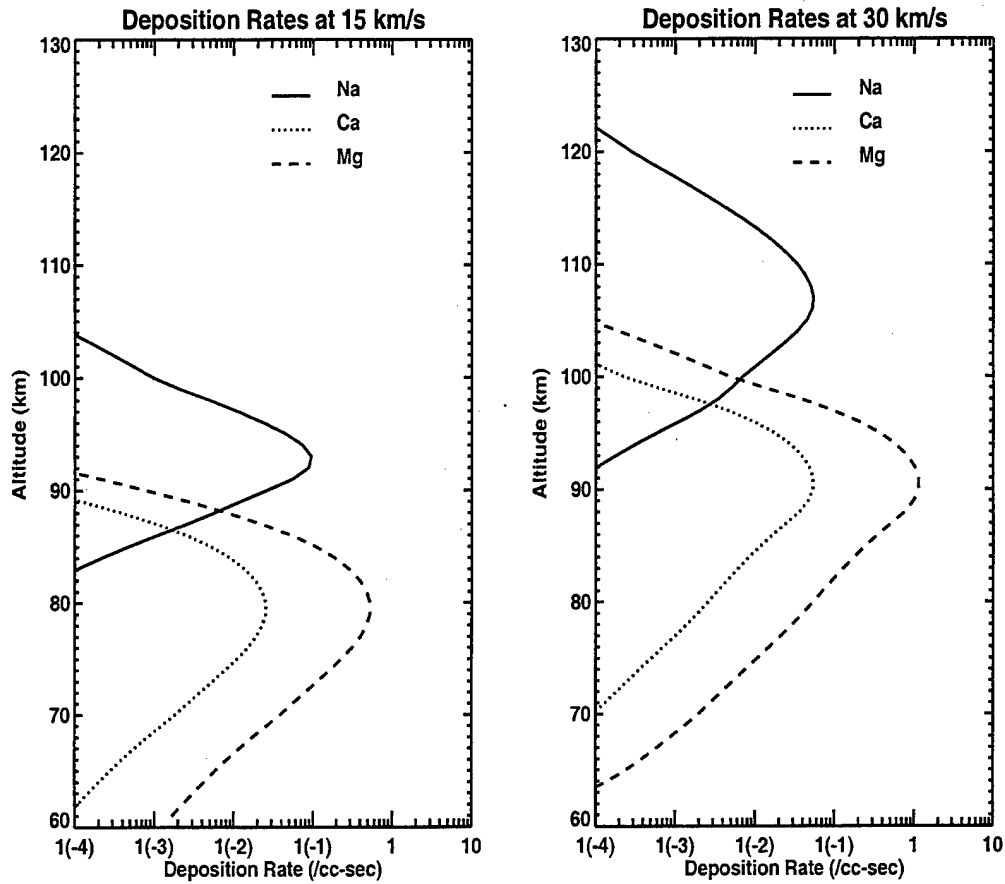


Figure 5. The deposition curves resulting from the differential ablation model for the three metals at incoming velocities of 12 km/sec (left) and 15 km/sec (right). Calcium is identical to magnesium but scaled down by 20.

For the slow particles, the calcium and magnesium ablation is at a rather low altitude, peaking at around 80 km. This is, of course, somewhat low compared to recent measurements by *Steel and Elford* [1991] who find 50 MHz radio meteors peaking at around 90 km instead. This disagreement leads us back to the issue of whether there is a large population of small, slow dust particles which are missed by the radio echo technique. The analysis of *Hughes* [1975] seems to suggest that this is a distinct possibility. In order for the present model to be very successful, it is necessary to postulate a relatively slow entry velocity for the majority of the dust particles contributing to the metal layers. There seems to be no evidence to date which would contradict this assumption.

Turning to the fast dust particles, calcium and magnesium ablation rates peak at around 90 km. Sodium ablation peaks at about 110 km. Ablation at altitudes as high as 140 km is evident in the *Steel and Elford* [1991] data at 2 MHz. Note that radio echo is completely insensitive to the metal species being ablated. Keep in mind that the ablation curves in Figure 5 arise from an admittedly simplistic model of differential ablation intended to investigate the possibility that differential ablation may explain the calcium depletion, and that the curves represent a single entry velocity. In the next section, these particles are applied to a kinetic model to show the impact of differential ablation on mesospheric abundances of the metal atoms and ions.

3. THE DYNAMIC MODEL

Deposition profiles from Section 2 are used in a time-dependent model including diffusion, ion transport and relatively comprehensive neutral and ion chemistry. The model follows closely that used for magnesium in *McNeil, et al.* [1996], considering two species only, the neutral and ionized metal. Steady state approximations are invoked for intermediate neutral and ion complexes. These approximations are valid as long as diffusion and transport are slow compared to the processes maintaining the steady state. These approximations have been verified through multi-component models which yield virtually the same results. The two-component models are used for computational efficiency and require the specification of three rates: the rate at which neutrals are converted into ions, r_c , the rate at which ions are destroyed to recreate

neutrals, r_d , and the rate at which neutrals are removed from the system by the sink, r_s .

The destruction rates of the neutrals are, of course, critical to the question of the relative abundances of the neutrals in the mesosphere and the details of the model warrant some attention in this regard. First, in order to use the two-component model, we must assume that the sink species is never reconverted into the neutral metal or metal complexes. Secondly, we have chosen a different sink species, NaHCO_3 for the sodium from that for the calcium for which we use CaCO_3 . This is a different calcium sink from that used for magnesium by *Plane and Helmer* [1995] who suggest that Mg(OH)_2 may be the primary sink for magnesium (and presumably for calcium as well). Based on their conclusions that a reduction of about 40 in the calcium deposition relative to the sodium is still needed with this sink species in order to match observations, we believe that the alternative sink species would make little difference in our results, since this is approximately the same reduction factor our model requires.

The full set of reactions used in the two-component model is given in Table 2. The footnotes accompanying that table provide sources of the rate coefficients used as well as some supplemental information. Units are /sec for uni-molecular reactions, /cc-sec for bi-molecular reactions and / cm^6 -sec for ter-molecular reactions. We will focus here on the differences between sodium and calcium in the chemical scheme.

TABLE 2. Kinetics of the Two-Component Models

#	Reaction	k(Na)	k(Ca)	k(Mg)
1	$M + O_2 + N_2 \rightarrow MO_2 + N_2$	$5.0(-30)^1$	$1.0(-30)^1$	$4.3(-36)^1$
2	$MO_2 + O \rightarrow MO + O_2$	$2.0(-14)^2$	$2.0(-14)^2$	$2.0(-14)^2$
3	$M + O_3 \rightarrow MO + O_2$	$6.0(-10)^1$	$3.0(-10)^1$	$3.0(-10)^1$
4	$MO + O \rightarrow M + O_2$	$2.2(-10)^3$	$2.2(-10)^3$	$2.2(-10)^3$
5a	$MO + CO_2 + N_2 \rightarrow MCO_3 + N_2$	n/a^4	$3.9(-27)^5$	$3.9(-27)^5$
5b	$MO + H_2O \rightarrow MOH + OH$	$1.2(-10)^1$	n/a^4	n/a^4
6b	$MOH + H \rightarrow M + H_2O$	$2.6(-12)^1$	n/a^4	n/a^4
7b	$MOH + CO_2 + N_2 \rightarrow MHCO_3 + N_2$	$1.9(-28)^1$	n/a^4	n/a^4
8	$M + hv \rightarrow M^+$	$1.7(-5)^6$	$3.5(-5)^6$	$4.0(-7)^6$
9	$M + O_2^+ \rightarrow M^+ + O_2$	$2.7(-9)^7$	$4.0(-9)^8$	$2.0(-9)^8$
10	$M + NO^+ \rightarrow M^+ + NO$	$2.8(-10)^7$	$1.0(-9)^8$	$8.1(-10)^8$
11	$M + O^+ \rightarrow M^+ + O$	$1.0(-11)^9$	$1.0(-9)^{10}$	$1.0(-9)^{10}$
12	$M^+ + e^- \rightarrow M + hv$	$4.0(-12)^{11}$	$4.0(-12)^{11}$	$4.0(-12)^{11}$
13	$M^+ + N_2 + O_2 \rightarrow MO_2^+ + N_2$	n/a^{12}	$6.6(-30)^{13}$	$2.5(-30)^{13}$
14	$MO_2^+ + e^- \rightarrow M + O_2$	n/a^{12}	$5.0(-7)^{13}$	$3.0(-7)^{13}$
15	$M^+ + O_3 \rightarrow MO^+ + O_2$	n/a^{12}	$1.6(-10)^{13}$	$2.3(-10)^{13}$
16	$MO^+ + e^- \rightarrow M + O$	n/a^{12}	$5.0(-7)^{13}$	$1.0(-7)^{13}$
17	$MO^+ + O \rightarrow M^+ + O_2$	n/a^{12}	$1.0(-10)^{13}$	$1.0(-10)^{13}$
18	$MO_2^+ + O \rightarrow MO^+ + O_2$	n/a^{12}	$1.0(-10)^{13}$	$1.0(-10)^{13}$
19	$M^+ + N_2 + N_2 \rightarrow M.N_2^+ + N_2$	$2.5(-30)^{14}$	$2.5(-32)^{15}$	$2.5(-32)^{15}$
20	$M.N_2^+ + e^- \rightarrow M + N_2 + N_2$	$3.0(-7)^{16}$	$3.0(-7)^{16}$	$3.0(-7)^{16}$

(Footnotes on Table 2)

- ¹ Measured rates [*Plane and Helmer*, 1994].
- ² In the two-component model, this reaction is assumed to be complete, since there are no competitors for MO_2 . The reported rate is an estimate for sodium from *Plane* [1991].
- ³ Measured rate [*Plane and Husain*, 1986] is used for the other two metals as well.
- ⁴ A different path is used as a sink mechanisms for Na than is used for Ca and Mg, the reasoning being that Rxn(5a) although it does obtain for Na is insignificant for when compared to Rxn(6) and that Rxn(6) does not obtain for Ca nor for Mg.
- ⁵ We use the rate measured for sodium by *Ager and Howard* [1986] for the other two metals.
- ⁶ Estimates of the photo-ionization rates are from *Swider* [1969].
- ⁷ These rates are the result of measurements recently completed by *Levandier et al.* [1997]
- ⁸ Extrapolations of high energy cross-sections [*Rutherford, et al.*, 1971] carried out by *Ferguson* [1972].
- ⁹ This rate was chosen to be slow in deference to observations [cf. *Rutherford, et al.*, 1971] that the reaction is too slow to measure.
- ¹⁰ These rates have been chosen to be near those for NO^+ based on comparisons of the high energy cross sections measured by *Rutherford, et al.* [1971,1972].
- ¹¹ Value for sodium from *Bates and Delgarno* [1962].
- ¹² These reactions have, to our knowledge, not been observed for sodium ion and are therefore not included in the kinetic model.
- ¹³ Values from *Aikin and Goldberg* [1973] and references cited therein.
- ¹⁴ This value was quoted to us by *J.M.C. Plane* privately [1996].
- ¹⁵ The species Mg.N_2^+ has been observed spectroscopically [*Robbins, et al.* 1995] and the rate of the reaction for magnesium has been estimated (see text).
- ¹⁶ As in (2) above, the chosen rate for Rxn(20) is irrelevant in the two-component model, since the result of Rxn(19) is assumed to be converted completely to the atomic species. The value is from *Aikin and Goldberg* [1973].

Beginning with the neutrals, both metals are converted to MO_2 ($\text{M} = \text{Na, Mg, Ca}$) through the three-body reaction with O_2 in Rxn(1). In the two-component model, we assume that all MO_2 is immediately converted to MO . The alternative would be recycling to the neutral metal through a reaction with atomic hydrogen [*Plane and Helmer*, 1994].

However, comparison of the rates shows that this is a minor pathway. As noted in Table 2, the chosen rate for Rxn(2) is therefore insignificant, since the model assumes complete and immediate conversion. MO is also formed by direct reaction with ozone through Rxn(3). The MO can be recycled to the atomic metal through Rxn(4) or for calcium and magnesium can be converted to MCO_3 through Rxn(5a). It is here that the journey ends for the calcium and magnesium neutral. Although Rxn(5a) does obtain for sodium, we find that a faster pathway is Rxn(5b) to form NaOH. The NaOH can then be recycled to atomic sodium through Rxn(6b) or the sodium can be lost to the sink $NaHCO_3$ through Rxn(7b). We have omitted the first pathway for simplicity, because the second pathway is the dominant one. The second pathway does not exist for either calcium or magnesium because $\{Ca,Mg\}HCO_3$ is not a stable species [Plane and Helmer, 1994].

Under these assumptions, the removal rate for calcium and magnesium is calculated by considering rates of creation of CaO and CaO_2 and the branching ratios that either return the metal to elemental form or carry it onward into the sink species.

$$r_{s,Ca} = (k_1[O_2][N_2] + k_3[O_3]) \frac{k_{5a}[CO_2][N_2]}{k_4[O] + k_{5a}[CO_2][N_2]} \quad (6)$$

The removal rate of sodium is a slightly more complicated expression due to the extra step involving NaOH.

$$r_{s,Na} = (k_1[O_2][N_2] + k_3[O_3]) \left(\frac{k_{5b}[H_2O]}{k_4[O] + k_{5b}[H_2O]} \right) \left(\frac{k_{7b}[CO_2][N_2]}{k_{6b}[H] + k_{7b}[CO_2][N_2]} \right) \quad (7)$$

The second and third bracketed terms in Eq(7) represent the fact that both Rxn(4) and Rxn(6b) return the metal to elemental form. Therefore, the product should result in the branching ratio between atomic neutral and sink species $NaHCO_3$.

The major and minor atmospheric constituents needed for calculation of the removal rates are taken from a variety of sources described in McNeil, *et al.* [1995]. Profiles for all atmospheric neutrals used in this model are shown in Figure 6. The resulting rates of removal are shown in Figure 7. Below about 80 km, there is a branch for each

species due to the day-to-night variation in atomic oxygen and hydrogen. The slower removal rate pertains to the day when Rxn(4) and to a lesser extent Rxn(6b) become more active, thus cutting down on the neutral destruction. What is interesting in Figure 7 is that the removal rate for neutral sodium is actually faster by a factor of about ten at all altitudes. This would lead to an excess of calcium rather than the observed excess of sodium. The depletion model must then overcome this tendency for sodium to be removed faster. The uncertainties in these rates could be substantial. However, it seems clear that the natural tendency is for sodium to be removed at a somewhat higher rate than calcium.

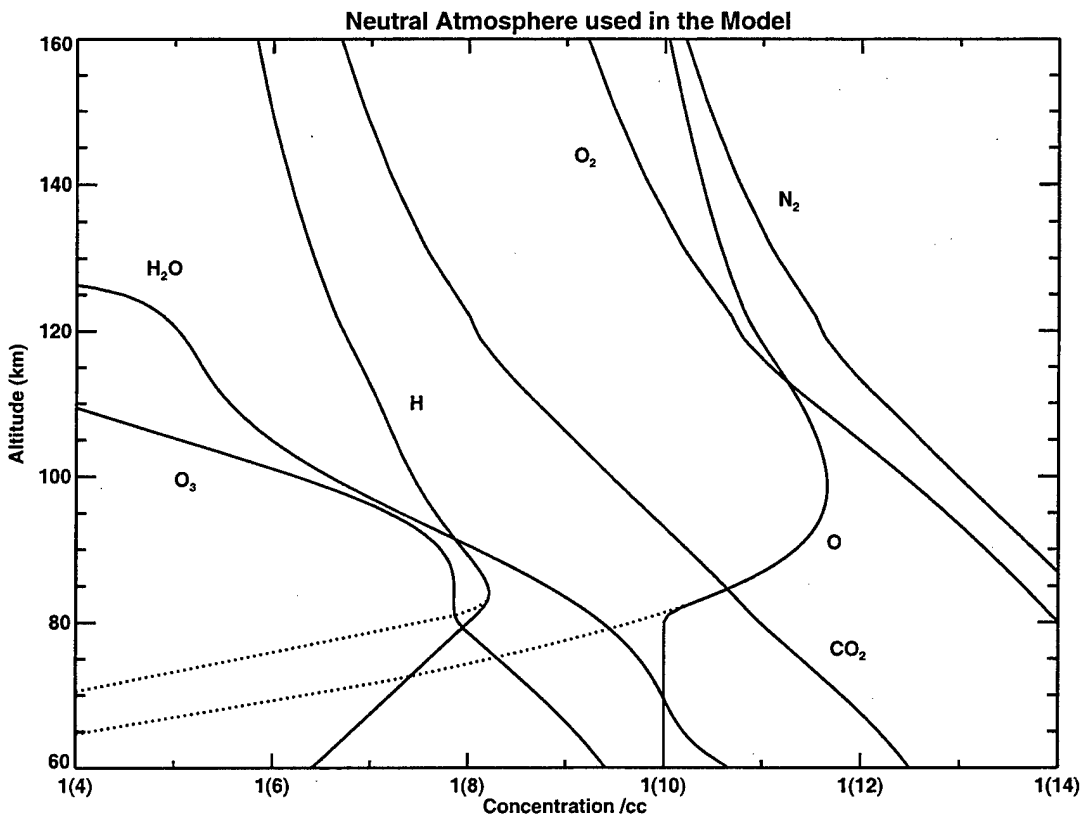


Figure 6. The model for neutral atmospheric components used in these calculations. Dashed curves indicate night values which are significantly different for O and H. Diurnal O₃ variation is not considered.

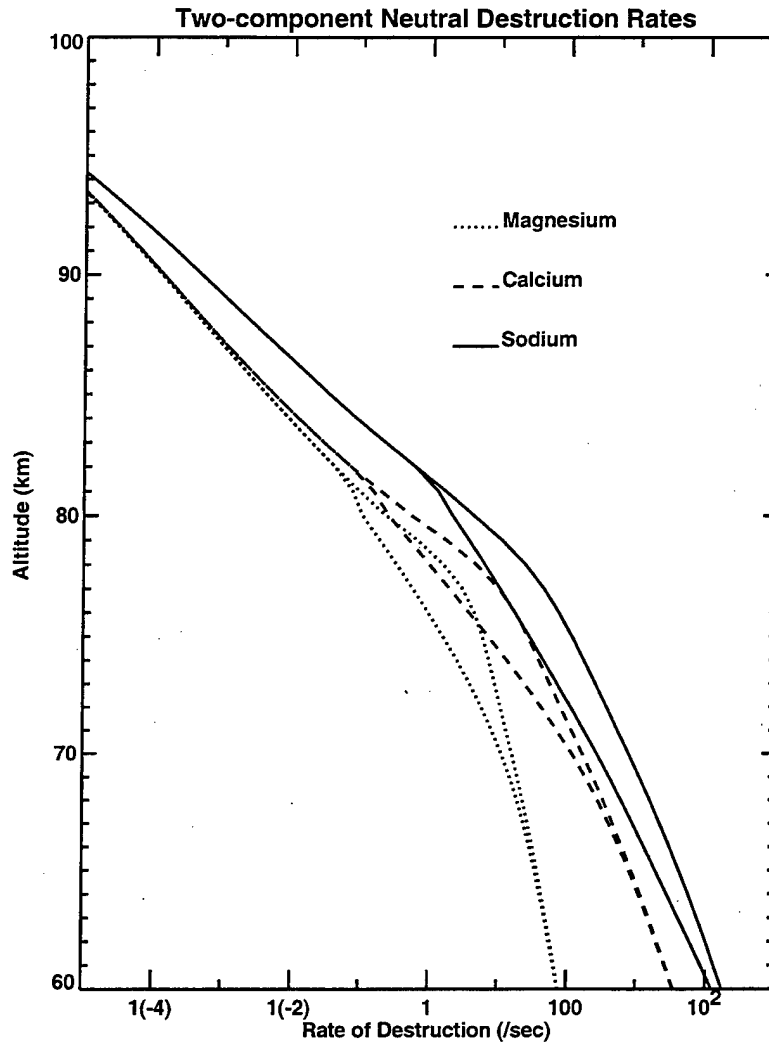


Figure 7. Removal rates for neutral metals computed from Eq(5) and Eq(6) and the rates in Table 2 for the two-component model. Note that the removal rate of sodium is *higher* than calcium, contrary to the calcium depletion.

Turning to the ions, Table 2 shows a somewhat different set of circumstances for sodium and the alkali earth metals. Ions are created in the model either through photoionization or through charge exchange with the major ionospheric species. The latter being the main mechanism for creation of the ions. The charge exchange cross sections have been measured at relatively high energies and extrapolated to mesospheric temperatures. Recently, *Levandier, et al.* [1997] have performed measurements and have concluded that the cross section for charge exchange between

sodium and O_2^+ is about an order of magnitude higher than generally assumed in early modeling. Similar results were obtained by *Farragher, et al.* [1969]. This puts the charge exchange rate for sodium more in line with that of calcium and magnesium as measured by *Rutherford, et al.* [1971]. The values used in this model reflect this similarity between the three metals studied. The charge exchange rates with NO^+ are also comparable for the three. As for exchange with O^+ , it would appear from comments in *Rutherford, et al.* [1971] that the exchange rate with Na is too small to be measured. Therefore, Rxn(11) has been assigned a small value for sodium. We find that this leads to a good amount of neutral sodium in the thermosphere, corresponding to observations of *Gardner, et al.* [1996]. Values for O^+ exchange with the other metals have been chosen to be near those for O_2^+ exchange based in the similarity apparent in the high energy cross sections of Rutherford. Succinctly, then, the mesospheric rates of ion creation in the model are basically the same for all three metals, O^+ being quite insignificant below perhaps 140 km.

The neutralization of the atomic ion, however, appears to be somewhat different between sodium and calcium. The rates for dielectronic recombination have been chosen to be the same. Dielectronic recombination is quite influential in the thermosphere in maintaining the density of neutral metals [*McNeil, et al.*, 1996] but does little to the mesospheric ion or neutral layers compared to three-body recombination. The three-body recombination processes differ both in the nature of the primary ion complex formed and in the recycling of the complex ion. Sodium ion forms NaN_2^+ quite readily [*Plane and Helmer*, 1994]. The MgN_2^+ complex has been observed [*Robbins, et al.* 1995] but the creation rate is unknown and experiments requiring the formation of Mg^+ are difficult to perform in the laboratory. It is our guess that the rate of MgN_2^+ formation is probably significant and we have attempted to roughly estimate the rate, or at least to calibrate the model, by comparing the model curves with measured Mg^+ densities compiled by *Grebowsky, et al.* [1997].

In Figure 8, the magnesium ion layer is plotted for four choices of rates of Rxn(19). There is obviously a great deal of scatter in the data due to many factors. However, it seems clear that the neglect of Rxn(19) does not give good agreement. It is also clear that using the same rate as for sodium gives a layer that is somewhat too high. A rate of $2.5(-32) /cm^6\text{-sec}$ was chosen because it seems to fit the data "best". In defense of this, note that the difference in rates for Rxn(19) for sodium and calcium does not have a major effect on the relative ion densities, although it does lead to a Ca-

II layer which is perhaps 5 km lower than the Na-II layer. Decreasing k_{19} from $2.5(-30)$ to $2.5(-31)$ / $\text{cm}^6\text{-sec}$ results in a factor of two increase in ion column density while further decreasing it to $2.5(-32)$ / $\text{cm}^6\text{-sec}$ results in a further increase by a factor of one-half. These changes are small when compared to the two orders of magnitude depletion in the neutrals. While the variation of this rate could vary the ion density by perhaps twenty at the extremes, a value was adopted which has some basis in measured data. In further defense of this rather rough treatment of kinetics, it is noted that until last year, the best value of k_{19} for sodium was a full order of magnitude lower than that in use here [Plane, 1996].

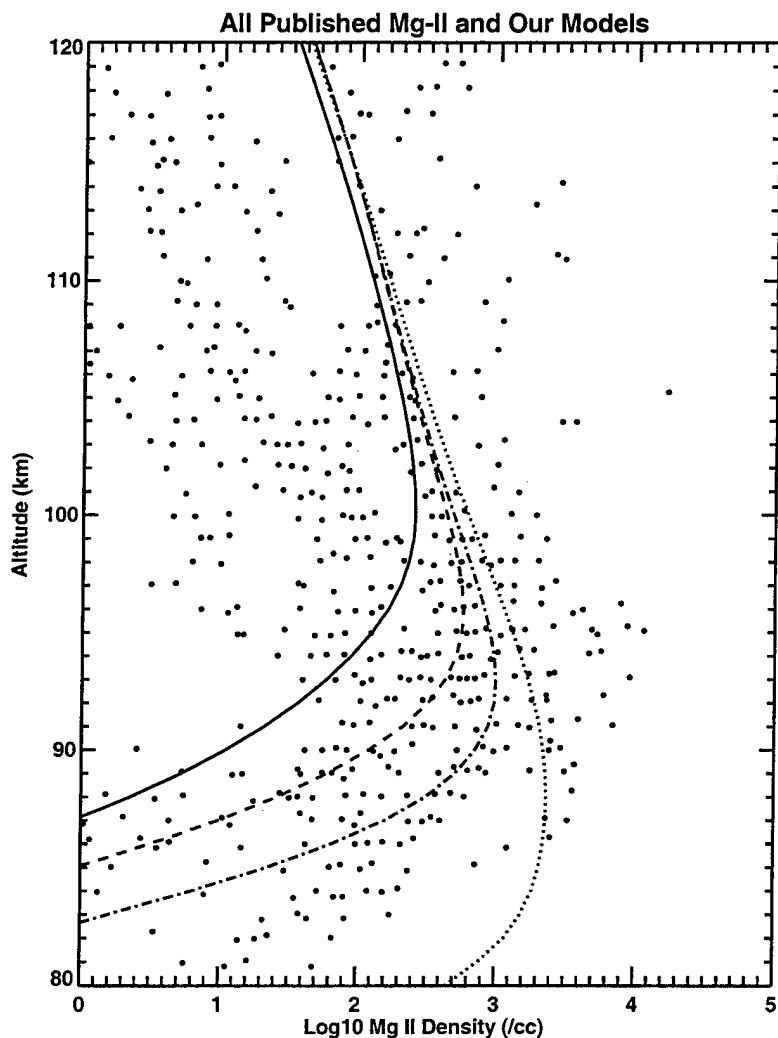


Figure 8. Comparison of the magnesium ion layer predicted by the model with the rate for Rxn(19) at 1(-30) (solid line), 1(-31) (dashed line), 1(-32) (dot-dash), and $0/\text{cm}^6\text{-sec}$ (dots) (top to bottom) as compared with published Mg^+ IMS [Grebowsky *et al.*, 1997].

Calcium and magnesium ions undergo a three body reaction to form MO_2^+ while sodium does not. These metals also form MO^+ by reaction with ozone, while sodium does not. Since the molecular ions are destroyed quite rapidly by molecular dissociative recombination (Rxn(14,16,20)) it might be expected that the calcium and magnesium ions would be neutralized faster than the sodium. However, CaO^+ is also converted back to the atomic ion through reaction with atomic oxygen and CaO_2^+ may be converted by reaction with atomic oxygen to CaO^+ . These recycling reactions back to Ca^+ dominate very strongly, as can be seen in the lower curve of Figure 8, which represents the ion layer with the oxygen and ozone pathways as the only sink. With Rxn(19) as the primary sink for these ions, however, the bottom line is that none of the ion chemistry with oxygen makes much difference in the resulting ion layer. Note that exclusion of Rxn(18), which has not to our knowledge been observed in the laboratory, is basically equivalent to including Rxn(19), since it provides a fast sink for the ions by cutting off the recycling pathway.

To underscore the present uncertainty in the mechanisms of these metal ion chemical pathways, note that it has recently been determined [Cox and Plane, 1997] that the NaN_2^+ complex undergoes a rapid ligand exchange with atomic oxygen. These authors suggest that the resulting NaO^+ is rapidly recycled to the ion. This would put us in the same situation as would using Rxn(18) without Rxn(19) for calcium and magnesium ion, were it not for the fact that NaN_2^+ also apparently undergoes ligand exchange with CO_2 [Cox and Plane, 1997] and does not undergo further rearrangement but rather is neutralized rapidly through molecular dissociative recombination with an electron. This means that there is a pathway available, equivalent although perhaps not equal in rate, to Rxn(19) which provides a three-body sink. We have tried the chemical scheme of Cox and Plane [1997] in the current sodium model and find that it leads to an ion layer quite similar to that obtained through the scheme in Table 2. It would therefore appear that a critical requirement for obtaining a reasonable sodium layer is merely a rapid three-body ion sink and that the precise mechanism is of secondary importance.

The rates of creation of the metal ions for the two-component model are given by the same expression for all the metal species.

$$r_{c,M} = k_8 + k_9[O_2^+] + k_{10}[NO^+] + k_{11}[O^+] \quad (8)$$

The rate expressions for destruction of the ions in the two-component model differ between sodium and the alkaline earth metals. The destruction of Na^+ is given by

$$r_{d,\text{Na}} = k_{12}[e^-] + k_{19}[\text{N}_2]^2 \quad (9)$$

since there is no recycling of NaN_2^+ back to the ion and since we assume that the ion complex is immediately neutralized by molecular dissociative recombination. The destruction of calcium and magnesium is given by a more complicated expression including branching representing the competition of recycling with recombination.

$$r_{d,\text{Mg,Ca}} = k_{12}[e^-] + k_{19}[\text{N}_2]^2 + k_{13}[\text{N}_2][\text{O}_2] \left(\frac{k_{14}[e^-]}{k_{14}[e^-] + k_{18}[\text{O}]} \right) + \left(\frac{k_{13}[\text{N}_2][\text{O}_2]}{k_{14}[e^-] + k_{18}[\text{O}]} \right) \left(\frac{k_{16}[e^-]k_{18}[\text{O}]}{k_{16}[e^-] + k_{17}[\text{O}]} \right) + k_{15}[\text{O}_3] \left(\frac{k_{16}[e^-]}{k_{16}[e^-] + k_{17}[\text{O}]} \right) \quad (10)$$

Eq(10) represents the two-branch process for CaO_2^+ . The first two terms in Eq(10) are identical to sodium. The third term represents MDR of the CaO_2^+ species with a branch representing the fraction which is transformed to CaO^+ . The third term represents the calcium ion that started the journey as CaO_2^+ then was converted to the monoxide then neutralized by MDR. The last term represents neutralization of the CaO^+ which was created from the direct reaction with ozone.

To conclude this section, the remainder of the modeling code will be briefly described. This is documented more thoroughly in *McNeil, et al.* [1996]. The model is fully time dependent in the sense that it solves the continuity equations for the neutral and ion species of each metal at a series of grid points from 60 to 600 km with a 1 km spacing. Molecular and eddy diffusion terms are included as is ion transport through the equatorial $\mathbf{E} \times \mathbf{B}$ drift. The electric field model is appropriate for the magnetic equator and is taken from *Richmond, et al.* [1980]. The electric fields do not effect the relative abundances of the metal ions or neutrals to any significant extent. They have been included and the model has been extended to high altitudes to examine the behavior of the model in the thermosphere as well as the mesosphere. The continuity equations are solved with 4-th order Runge-Kutta beginning with a complete absence of neutrals and ions. The model is run for ten days at one-second steps, at which point

the profiles are well converged and identical from day-to-day. What is left is a diurnal profile of the metals as a function of local time and altitude.

4. RESULTS

There are several inputs to the model that cannot be definitively determined at this time. If one accepts the deposition model described in Section 2 and the chemical scheme from Section 3, we are left with essentially only two variable parameters of any significance. These variables are the total influx of meteoric material and the velocity or distribution of velocities of the incoming particles. We can dispense with the first of these readily. The total influx is introduced into the model through a scale factor α which multiplies the deposition function curves in Figure 5. The same value of α is used for all three metals and the deposition function for magnesium is scaled up additionally by a factor of twenty to represent the meteoric abundance of the metal. By adjusting α we can achieve any desired column density for one of the species. Then, by using the same value for the other two metals, we can compare the relative column densities predicted by the model. Although it is not perhaps an obvious result, we find that both neutral and ion column densities scale linearly with α through a wide range of resultant column densities. This is convenient in that any choice of α will give rise to the same relative densities between the three metals. We choose α so as to give a sodium neutral column density of $5(9) \text{ cm}^{-2}$ which is a typical value [Simonich, *et al.*, 1979].

Turning to the variation of the model with incoming dust particle velocity, we note first that at all velocities, sodium is ablated almost completely. This result is in accord with experimental evidence. *Brownlee* [1985] describes analysis of particles collected from the deep sea. He finds that the composition of the bulk of the stony spheres collected is essentially chondritic in nature, except that the Na appears to be completely absent. The present model predicts that the remnant meteoric particle would be depleted in Na while retaining the less volatile elements in essentially the original proportion, as *Brownlee* finds. The model produces a remnant dust particle of the same basic nature as extraterrestrial particles collected on the Earth.

What is perhaps surprising is that the model predicts that a great deal of the calcium is also ablated. At 30 km/sec entry velocity the ratio of ablated sodium to calcium is near unity. Even at 12 km/sec we find that only about one-third of the original calcium

remains in the cosmic dust particle overall. This means that simple enrichment, that is, the process whereby the calcium just does not get out, could explain only a depletion of three in the mesospheric sodium to calcium to sodium ratio. This is to be compared to measured results of somewhere near two orders of magnitude. Although the remnant meteorite is enriched greatly in calcium, compared to sodium, this is only because the majority of the sodium is gone.

It is clear that the lack of ablation of the calcium cannot explain the two orders of magnitude depletion of calcium observed in the mesospheric layers. We find that the model predicts a substantially larger depletion than would be expected from enrichment alone. This is attributed to the fact that the calcium is deposited at a substantially lower altitude than is the sodium. At low altitudes, the processes removing the metal from the system are substantially faster than at higher altitudes. To examine the depletion predicted by the model, we have performed a parametric study on the relative mesospheric column densities of neutrals and ions as a function of incoming velocity. The results are shown in Table 3.

TABLE 3. Model Column Densities		
Incoming Velocity	Na/Ca	Na ⁺ / Ca ⁺
50 km/sec	2.1	1.4
30 km/sec	2.6	1.6
20 km/sec	8.0	5.4
15 km/sec	79.0	58.6
12 km/sec	699	704
11 km/sec	2345	2930
Measured	100	3

The table shows several interesting features. First, at velocities above 30 km/sec both the neutral and ion column density ratios remain unchanged. This is due to the fact that all of the sodium and calcium is ablated well above the altitude where the neutral sink processes become dominant. The reason that the neutral and ion abundance ratios are not unity is due primarily to the differences in the ion chemistry between sodium

and calcium with the ion mechanisms favoring the calcium ion as opposed to the sodium neutral. Also, the neutral calcium is slightly depleted, not from enrichment, but most likely because the calcium is still deposited lower in the atmosphere, nearer the altitudes where the neutral sink become significant.

The effect of Rxn(19) can also be examined through the high velocity depletions in the ions. The calcium ions are depleted slightly less than are the neutrals. An enhancement of perhaps 50% can be seen in the calcium ions over the sodium ions when neutral sodium is about twice as abundant. If the ion chemistry were identical, one would expect about twice as many sodium ions as calcium. This is roughly in agreement with the comparisons made for magnesium in Section 2. It shows that the choice of rate for Rxn(19) does not impact the results too strongly.

Table 3 shows that low velocity dust particles produce a strong enhancement in sodium relative to calcium at low incoming velocities. This is much higher than the factor of three that can be explained through enrichment. As alluded to above, the primary mechanism for calcium depletion appears to be the deposition of the calcium at lower altitudes than the sodium. This situation is shown schematically in Figure 9. A dashed line is drawn at the point where the rate of neutral recycling about equal, the rate of conversion into the sink species. In actuality, this transition is rather sharp and the concept of a "three-body line" below which the ablated metal is drawn immediately into the sink is a realistic analogy for the model's behavior. At 30 km/sec, the majority of the sodium and calcium deposition is above the three-body line, therefore differential ablation has no effect save for the small fraction of calcium that is unablated. At 12 km/sec entry velocity, however, the majority of the calcium is ablated below the three-body line while all of the sodium is ablated above this line. About one-third of the calcium remains unablated but the majority of that which is ablated is immediately removed from the system through the neutral sink. The sodium at 12 km/sec is also deposited nearly at the center of the mesospheric layer while the bulk of the calcium is deposited below the layer peak. Diffusion would therefore push the newly deposited calcium down into the sink region in a shorter time and diffusion is needed to push the calcium back up into the layer. Also, since the sodium is deposited higher, it has more time to be converted to ionic form giving it overall a longer lifetime relative to calcium. Conceptually, though, the penetration of the deposition into the sink region appears to be the major contributor to calcium depletion in the mesosphere.

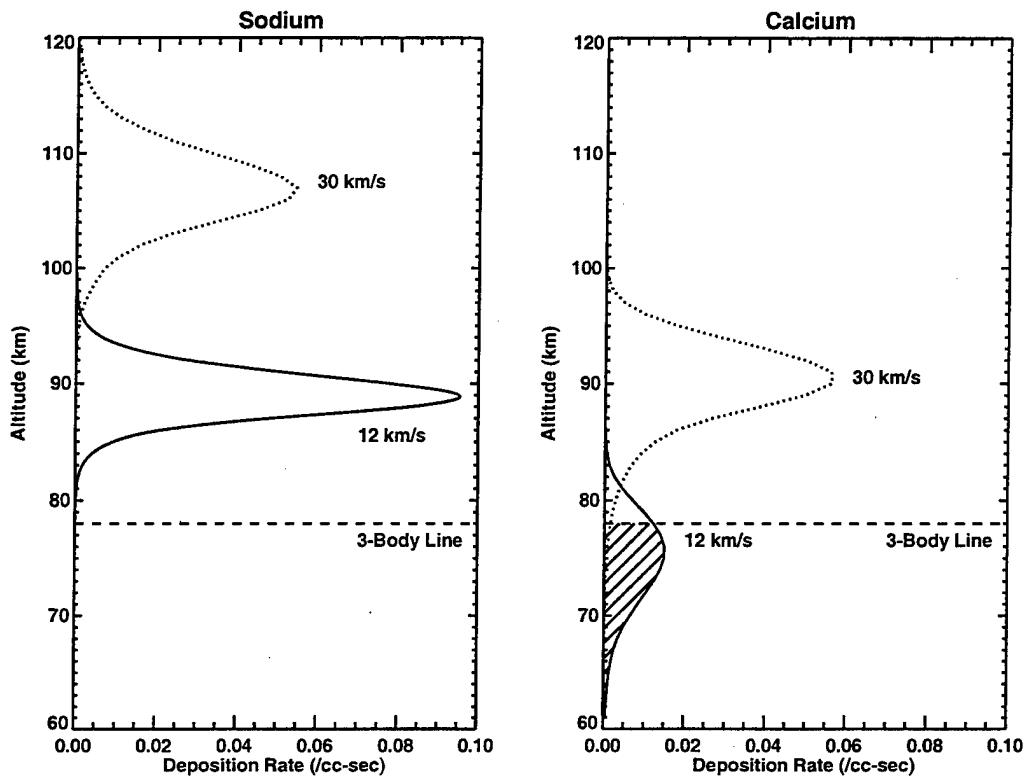


Figure 9. Illustration of the primary mechanism for calcium depletion comparing the altitude of deposition of sodium (right) with calcium (left) as they relate to the altitude where the sink becomes dominant.

What is perhaps more striking in Table 3 is that the ratio of neutral sodium to calcium is in good agreement with measurements for low velocity particles while the ion column density ratios are incorrect for the low velocity particles but nearer the measured result for the fast cosmic dust. In fact, as one might expect, the depletion in neutrals and ions follow each other quite closely for a single incoming velocity. It would be tempting to assume that all cosmic dust entered the atmosphere at 15 km/sec since this would give good agreement for the neutral calcium depletion measurements. However, such an assumption would give a model prediction for mesospheric ions far in excess of the measurements. Said another way, deposition of calcium and magnesium at altitudes too low leads to an under abundance of the ions of these metals. The assumption of a low incoming velocity also has severe ramifications in the

thermosphere, in that a population made up completely of low velocity particles would imply a severe lack of thermospheric ions.

Several optical measurements [*Gérard and Monfils.*, 1974; *Fesen and Hays*, 1982; *Gardner, et al.*, 1996] have found substantial densities of Mg^+ in the at the geomagnetic equator at altitudes above 200 km. Modeling studies [*Fesen, et al.*, 1983; *McNeil, et al.*, 1996] have successfully reproduced these features indicating magnesium ion densities on the order of 20-200 /cc. However, the model evaluated at 15 km/sec entry velocity or at slower velocities gives very little high altitude magnesium ion. This is simply because the metal is deposited too low to ever get a substantial amount of it above the mesosphere.

One solution which immediately comes to mind is to assume two different populations of incoming particles. This seems a reasonable route to take because the Earth is indeed surrounded by a substantial cloud of dust [*McDonnell*, 1980; *Brownlee*, 1985]. There is some debate on whether this dust is of asteroidal or cometary origin. However, even if the origin is from comets, cometary ejecta in the size range of 1-100 μm would be strongly subjected to the Poynting-Robertson effect, by which the radiative dispersion of solar photons saps energy from the dust particles over the eons and thereby tends to circularize their orbits. These dust particles would orbit the Sun with the Earth and would enter the atmosphere at the escape velocity of 11 km/sec. Particles in this size range are just those that contribute most strongly to the Earth's metal layers, as discussed in Section 2. The relative population of these particles is quite unknown since they are too slow and too small to be measured by radio echo [*Hughes*, 1975]. Therefore, it is proposed that there is a large and relatively constant influx of slow dust particles and also a smaller influx of faster particles corresponding presumably to the sporadic meteors which are routinely observed and arising from younger cometary swarms.

A parametric study has been performed assuming that the fast particles make up either 5% or 2% of the entire dust influx. Results are shown in Table 4 for a variety of choices for the slow and fast dust velocities. There are several possibilities that give results quite close to the measurements, especially if one admits that there may be other contributors to the calcium depletion aside from differential ablation. It is seen that the choice of the slow velocity tends to control the neutral ratios while the fast velocity controls the ions. With 95% of the dust at 12 km/s and 5% at 60 km/sec,

one finds a depletion of about twenty in the neutral calcium with good ion ratios. The best choice appears to be with 98% at 11 km/sec and 2% at 60 km/sec which produces a calcium reduction of a factor of forty, also with good ion ratios. The ion and neutral profiles from this case are shown in Figure 10. In the end, though, the fact that one arrives at some reasonably good agreement with several different choices gives one some confidence that the differential ablation concept is sound.

TABLE 4. Parametric Study of Neutral and Ion Ratios

Percent Fast Dust	Slow Dust Velocity (km/s)	Fast Dust Velocity (km/s)	Ratio of Na-I to Ca-I	Ratio of Na-II to Ca-II	Ratio of Mg-II to Na-II
5%	11	40	16.4	2.6	7.0
5%	11	50	16.5	2.2	8.2
5%	11	60	16.6	2.0	9.3
5%	12	40	22.5	3.4	5.3
5%	12	50	22.5	2.8	6.4
5%	12	60	22.9	2.5	7.3
5%	15	40	24.7	5.7	3.1
5%	15	50	25.7	4.7	3.9
5%	15	60	26.0	4.2	4.4
2%	11	40	38.2	4.4	4.0
2%	11	50	39.2	3.6	5.0
2%	11	60	40.0	3.2	5.7
2%	12	40	52.8	6.5	2.8
2%	12	50	50.2	5.3	3.4
2%	12	60	53.9	4.6	4.0
2%	15	40	43.1	11.3	1.6
2%	15	50	43.2	9.9	1.8
2%	15	60	43.4	8.2	2.2
	Measured	Results	100	3	8

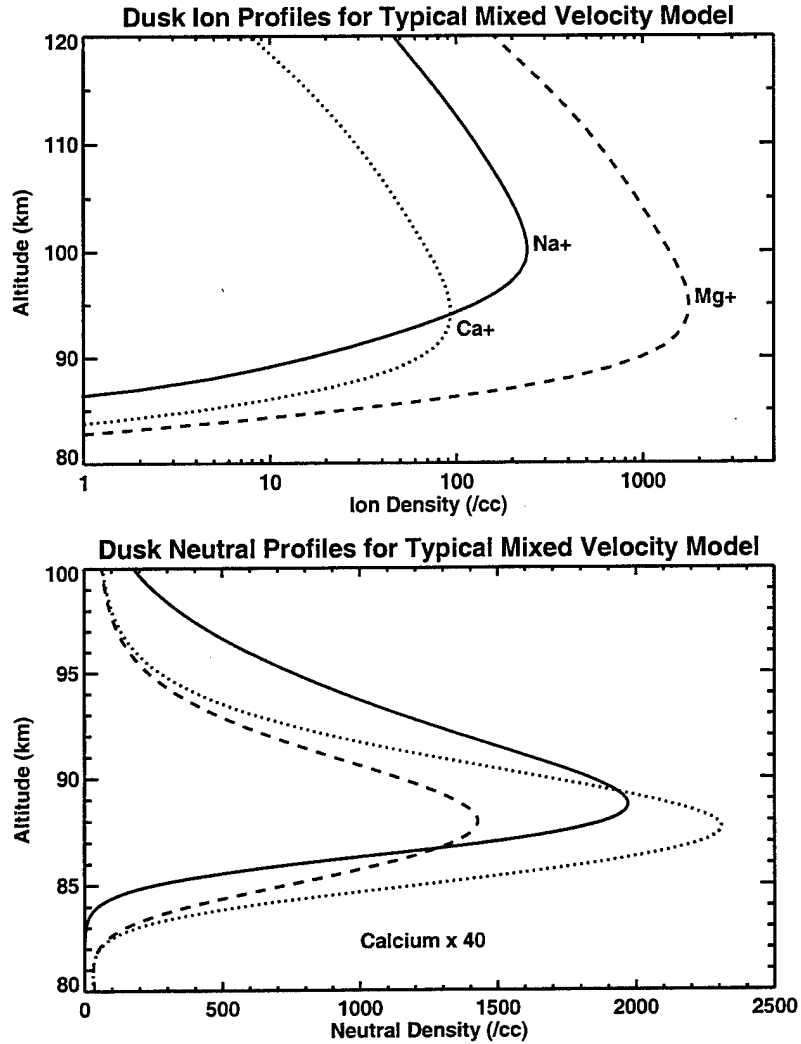


Figure 10. Mesospheric ion and neutral layers resulting from a mixture of 2% fast and 98% slow meteoric dust particles taken at dusk.

Examining the neutral layers first, the peak neutral densities for sodium and magnesium are approximately the same while the model of *Plane and Helmer* [1995] gives a magnesium layer which is smaller than the sodium layer by about a factor of five. *Plane and Helmer* [1995] use an alternative sink mechanism involving $Mg(OH)_2$, which could easily explain the difference. There is as yet no measured magnesium layer with which to compare. The peak in calcium density is about thirty times smaller than the sodium peak. *Qian and Gardner* [1995] find through simultaneous lidar measurements of Na and Ca that a factor of twenty-five is roughly the ratio of the peak calcium to sodium density while we arrive at a value of about thirty. One substantial difference

between the layers of *Qian and Gardner* [1995] and our model layers is that the former are closer to each other in peak altitude and overall shape while our calcium peak is about 1 km lower than the sodium peak with also a lower top and bottom-side. This suggests that the model removal rates may be somewhat incorrect. If the sodium removal rate were closer to the calcium removal rate (*c.f.* Figure 7) this would lower the bottom-side of the sodium layer and also increase the depletion ratio between sodium and calcium neutrals, bringing closer agreement with the measurements.

Turning to the ions, the *Plane and Helmer* [1995] model agrees with the present one in predicting a sodium ion peak near 100 km compared with an magnesium ion peak around 90 km. That the sodium ion peak is actually somewhat higher than that for magnesium is, at least, suggested by several rocket results [*Aikin and Goldberg*, 1973; *Kopp and Hermann*, 1983]. These also suggest a magnesium ion peak around 92 km, which is quite close to our result. The absolute column density of magnesium ion is predicted by the model to be about $1(10) / \text{cm}^2$ while *Anderson and Barth* [1971] find it to be closer to $4(9) / \text{cm}^2$. The peak magnesium ion density is about 2,000 /cc which is consistent with ion mass spectrometry measurements [*Aikin and Goldberg*, 1973; *Kopp and Hermann*, 1983]. Both of these are scalable parameters in the model, but recall that they correspond to a previously chosen column density for the sodium neutrals of $5(9) / \text{cm}^2$ so that these comparisons do have some meaning.

5. SUMMARY

This report presents a model which attempts to reproduce observed mesospheric metal densities and ratios for sodium, calcium and magnesium ions and neutrals. The basis of the model is that sodium is vaporized first before the other two metals begin to be deposited. Depletion of neutral calcium is found to arise from two sources, both the incomplete volatilization of the calcium and the deposition of the calcium at substantially lower altitudes than the sodium. The first of these leads to the deposition of more sodium than calcium. The second leads to a faster removal of the calcium metals. It appears, too, that the differences in ion chemistry between alkali and alkaline earth metals may contribute to the calcium depletion, with the slower removal rate of the ions contributing perhaps a factor of two to the far less severe depletion in calcium and magnesium ions. The depletion in the magnesium neutral layer is unknown, but do to similar chemistries, it is likely to be similar to that of calcium.

For the model to be very successful, we must assume that the vast majority of the dust enters the atmosphere at around 11 km/sec. This is a topic of much debate but there is reason to suspect that this is at least possible. We find, all things considered, that the model gives a strong calcium depletion with reasonable ion ratios for a variety of velocity distributions. The assumption that the vast majority of particles which contribute to the metal layers are slow is plausible in light of the arguments set forth. It is interesting that the model, in a sense, predicts the existence of these small, slow dust particles which are unmeasurable by current methods.

Comparisons of the resulting mesospheric layers have been made to several measurements. Overall, the agreement with observations is quite good, considering the comprehensive nature of the model. This model is an attempt to derive the relative ratios and absolute values of the three metals and metal ions beginning with a single value of cosmic dust influx and invoking plausible assumptions about cosmic dust and how it ablates in the atmosphere. While one must consider that there are many assumptions involved, as well as many variables which are poorly known, the success of the model suggests that differential ablation is adequate to explain a good portion of the depletion in the calcium layer relative to sodium.

6. REFERENCES

- Ager, J. W., III, and C. J. Howard, The kinetics of $\text{NaO} + \text{O}_2 + \text{M}$ and $\text{NaO} + \text{CO}_2 + \text{M}$ and their role in atmospheric sodium chemistry, *J. Geophys. Res.*, **13**, 1395, 1986.
- Aikin, A. C. and R. A. Goldberg, Metallic ions in the equatorial ionosphere, *J. Geophys. Res.*, **78**, 734, 1973.
- Anderson, J. G. and C. A. Barth, Rocket investigation of the Mg I and Mg II dayglow, *J. Geophys. Res.*, **76**, 3723, 1971.
- Bates, D. R. and A. Dalgarno, Electric recombination, in *Atomic and Molecular Processes*, D.R. Bates, ed., p. 245, Academic Press, New York, 1962.
- Blamont, J. E., Nouvelle méthode d'observation de l'émission atmosphérique des raies D du sodium, *C. R. Acad. Sci.*, **237**, 1320, 1953.
- Brownlee, D. E., Cosmic dust: Collection and research, *Ann. Rev. Earth Planet. Sci.*, **13**, 147, 1985.
- Brownlee, D. E., B. Bates and L. Schramm, The elemental composition of stony cosmic spherules, *Meteoritics & Planet. Sci.*, **32**, 157, 1997.
- Chapman, S., Notes on atmospheric sodium, *Astrophys. J.*, **88**, 164, 1938.
- Cox, R. M. and J. M. C. Plane, An ion-molecule mechanism for the formation of neutral sporadic Na layers, *J. Geophys. Res.*, ALOHA/ANLC-93 Special Issue, *submitted for publication*, 1997.
- Drowart, J., G. Exsteen, and G. Verhaegen, Mass spectrometric determination of the dissociation energies of the molecules MgO, CaO, SrO and Sr₂O, *Trans. Faraday Soc.*, **60**, 1920, 1964.
- Farragher, A. L., J. A. Peden and W. L. Fite, Charge transfer of N_2^+ , O_2^+ and NO^+ to sodium atoms at thermal energies, *J. Chem. Phys.*, **50**, 287, 1969.
- Fegley, B., Jr., and A. G. W. Cameron, A vaporization model for iron/silicate fractionalization in the mercury proto-planet, *Earth and Planet. Sci. Lett.*, **82**, 207, 1987.
- Ferguson, E. E. and F. C. Fehsenfeld, Some aspects of the metal ion chemistry of the Earth's atmosphere, *J. Geophys. Res.*, **73**, 6215, 1968.

- Ferguson, E. E., Atmospheric metal ion chemistry, *Radio Sci.*, **7**, 397, 1972.
- Fesen, C. G. and P. B. Hays, Mg⁺ morphology from Visual Airglow Experiment observations, *J. Geophys. Res.*, **87**, 9217, 1982.
- Fesen, C. G., P. B. Hays and D. N. Anderson, Theoretical modeling of low latitude Mg⁺, *J. Geophys. Res.*, **88**, 3211, 1983.
- Gardner, J. R., A. Viereck, E. Murad, S. T. Lai, D. Knecht, C. P. Pike, L. Broadfoot, E. Anderson, W. Sandel, and W. J. McNeil, Mg⁺ and other metallic emissions observed in the thermosphere, *Adv. Space Res.*, **18**, 61, 1996.
- Gardner, C. S., T. J. Kane, D. C. Senft, J. Qian and G. C. Papen, Simultaneous observations of sporadic E, Na, Fe, and Ca⁺ layers at Urbana, Illinois: Three case studies, *J. Geophys. Res.*, **98**, 16,865, 1993.
- Gerard, J. C. and A. Monfils, Satellite observations of the equatorial MgII dayglow intensity distribution, *J. Geophys. Res.* **79**, 2455, 1974.
- Granier, C. P., J. P. Jegou and G. Megie, Atomic and ionic calcium in the upper atmosphere, *J. Geophys. Res.*, **94**, 9917, 1989.
- Grebowsky, J. M. and H. C. Brinton, Fe⁺ ions in the high latitude F-region, *Geophys. Res. Lett.*, **5**, 791, 1978.
- Grebowsky, J. M. and M. W. Pharo, III, The source of mid-latitude metallic ions at F-region altitudes, *Planet. Space Sci.*, **33**, 807, 1985
- Grebowsky, J. M., W. D. Pesnell and R.A. Goldberg, What meteor showers can be expected to have the most impact on the ionosphere?, *presented at the 1997 Spring Meeting of the American Geophysics Union, Baltimore, Md, to be published, 1997.*
- Hanson, W. B. and S. Sanatani, Meteoric ions above the F₂ peak, *J. Geophys. Res.*, **75**, 5505, 1970.
- Hughes, D. W., Cosmic dust influx to the earth, *Space Res.*, **XV**, 1975.
- Hughes, D. W., The Meteorite Flux, *Space Sci. Rev.*, **61**, 275, 1992.
- Hughes, D. W., *Private Communication*, 1997.
- Kane, T. J. and C. S. Gardner, Structure and variability of the night-time mesospheric Fe layer at midlatitudes, *J. Geophys. Res.*, **98**, 16,875, 1993.

- Kelley, M. C., *The Earth's Ionosphere, Int. Geophys. Ser.*, **43**, Academic Press, San Diego, Calif., 1989.
- Kopp, E. and U. Herrmann, Ion composition of the lower ionosphere, *Annales Geophysicae*, **2**, 83, 1984.
- Kopp, E., On the abundance of metal ions in the lower ionosphere, *J. Geophys. Res.*, **102**, 9667, 1997.
- Langmuir, I., The vapor pressure of metallic tungsten, *Phys. Rev.*, **2**, 329, 1913.
- Levandier, D. J., R. A. Dressler, S. Williams and E. Murad, A high-temperature guided-ion beam study of $\text{Na} + \text{X}^+$ ($\text{X} = \text{O}_2, \text{NO}, \text{O}$) charge transfer reactions, *Faraday Trans.*, **93**, 2611, 1997.
- Love, S. G. and D. E. Brownlee, Heating and thermal transformation of micrometeoroids entering the Earth's atmosphere, *Icarus*, **89**, 26, 1991.
- Love, S. G. and D. E. Brownlee, A direct measurement of the terrestrial mass accretion rate of cosmic dust, *Science*, **262**, 550, 1993.
- Mason, B., *Handbook of Elemental Abundances in Meteorites*, Goodman and Breech, New York, 1971.
- McDonnell, J. A. M., Microparticle studies by space instrumentation, in *Cosmic Dust*, J. A. M. McDonnell, ed., John Wiley & Sons, New York, p.377, 1980.
- McNeil, W. J., E. Murad and S. T. Lai, A comprehensive model for the atmospheric sodium layer, *J. Geophys. Res.*, **100**, 16847, 1995.
- McNeil, W. J., S. T. Lai and E. Murad, A model for meteoric magnesium in the ionosphere, *J. Geophys. Res.*, **101**, 5251, 1996.
- McNeil, W. J., S. T. Lai and E. Murad, Models of thermospheric sodium, calcium, and magnesium at the magnetic equator, *Adv. Space Res.*, in press, 1997.
- Megie, G. and J. E. Blamont, Laser sounding of atmospheric sodium: interpretation in terms of global atmospheric parameters, *Planet. Space Sci.*, **25**, 1093, 1977.
- Notsu, K., N. Onuma, N. Nishida and H. Nagasawa, High temperature heating of the allende meteorite, *Geochim. Cosmochim. Acta*, **42**, 903, 1978.

- Papanastassiou, D. A., G. J. Wasserburg and D. E. Brownlee, Chemical and isotopic study of extraterrestrial particles from the ocean floor, *Earth Planet. Sci.*, **64**, 341, 1983.
- Plane, J. M. C. and D. Husain, Determination of the absolute rate constant for the reaction $O + NaO \rightarrow Na + O_2$ by time-resolved atomic chemiluminescence at 589 nm, *J. Chem. Soc. Faraday Trans.*, **82**, 2047, 1986.
- Plane, J. M. C., The chemistry of meteoric metals in the Earth's upper atmosphere, *International Reviews in Physical Chemistry*, **10**, 55, 1991.
- Plane, J. M. C. and M. Helmer, Laboratory studies of the chemistry of meteoric metals, *Research in Chemical Kinetics*, **2**, 313, 1994.
- Plane, J. M. C. and M. Helmer, Laboratory study of the reactions $Mg + O_3$ and $MgO + O_3$: Implications for the chemistry of magnesium in the upper atmosphere, *Faraday Discuss.*, **100**, 1, 1995.
- Plane, J. M. C., An explanation for the depletion of calcium in the upper atmosphere, *IUGG XXI General Assembly*, 1995 (abstract only).
- Qian, J. and C. S. Gardner, Simultaneous lidar measurements of mesospheric Ca, Na and temperature profiles at Urbana, Illinois, *J. Geophys. Res.*, **100**, 7453, 1995.
- Richmond, A. D., M. Blanc, B. A. Emery, R. H. Wand, B. G. Fejer, R. F. Woodman, S. Ganguly, P. Amayenc, R. A. Behnke, C. Calderon and J. V. Evans, An empirical model of quiet-day ionospheric electric fields at middle and low latitudes, *J. Geophys. Res.*, **85**, 4658, 1980.
- Robbins, D. L., L. R. Brock, J. S. Pilgrim and M. A. Duncan, Electron spectroscopy of the Mg^+N_2 complex: Evidence for photoinduced activation of N_2 , *J. Chem. Phys.*, **102**, 1481, 1995.
- Rutherford, J. A., R. F. Mathis, B. R. Turner and D. A. Vroom, Formation of magnesium ions by charge transfer, *J. Chem. Phys.*, **55**, 3785, 1971.
- Rutherford, J. A., R. F. Mathis, B. R. Turner and D. A. Vroom, Formation of calcium ions by charge transfer, *J. Chem. Phys.*, **57**, 3087, 1972.
- Simonich, D. M., B. R. Clemesha and V. W. J. K. Kirchoff, The mesospheric sodium layer at 23° S: Nocturnal and seasonal variations, *J. Geophys. Res.*, **84**, 1543, 1979.

Steel, D. L. and W. G. Elford, The height distribution of radio meteors: comparison of observations at different frequencies on the basis of standard echo theory, *J. Atmos. Terr. Phys.*, **53**, 409, 1991.

Swider, W., Jr., Processes for meteoritic elements in the E region, *Planet. Space Sci.*, **17**, 1233, 1969.

Zbinden, P. A., M. A. Hidalgo, P. Eberhardt and J. Geiss, Mass spectrometer measurements of the positive ion composition in the D- and E-regions of the ionosphere, *Planet. Space Sci.*, **23**, 1621, 1975.